

RESULTS

Characteristics of the patients and nodules

A TOTAL OF 127 patients were enrolled, of whom 26 had chronic HBV infections and 101 had HCV infections, and 68 had virus-associated cirrhosis. No statistically significant differences in the initial clinical characteristics were found between the non-clean liver and clean liver groups (Table 1). Thirty-five hypovascular hypointense nodules were found in 18 patients in the non-clean liver group (1–5 nodules per patient) at baseline (data not shown). Twenty-four of these 35 nodules were detectable only on the hepatocyte phase MRI and were undetectable by US, CT and non-hepatocyte phase MRI. None of the 35 nodules showed high intensity on T2WI. The median nodule diameter was 8 mm (range, 4–13 mm; 33 nodules with ≤ 10 mm, two nodules with 12 mm and 13 mm).

HCC incidence according to initial MRI findings

Hepatocellular carcinoma was diagnosed in 17 patients, 10 in the non-clean liver group and seven in the clean liver group; 14 of these patients had HCV infection. Thirteen patients were diagnosed according to the AASLD imaging criteria.¹⁹ Four patients were diagnosed pathologically by liver biopsies that were performed, based on enlargement of the nodules of more than 10 mm in diameter during the observation period.

The cumulative 1-, 2- and 3-year HCC incidence rates were 1.5%, 10.2% and 13.4%, respectively. As determined by the Kaplan–Meier method, these rates were 11.1% (95% confidence interval [CI], 0.0–25.6%), 38.8% (95% CI, 16.3–61.4%) and 55.5% (95% CI, 32.6–78.5%) in the non-clean liver group, and 0.0% (95% CI, 0.0–2.3%), 5.5% (95% CI, 0.0–9.8%) and

6.4% (95% CI, 1.8–11.0%) in the clean liver group; the former group showed significantly higher rates of development of typical HCC than the latter ($P < 0.001$) as shown in Figure 2. The median imaging intervals were 3 months (range, 3–6) in the non-clean liver group and 4 months (range, 2–12) in the clean liver group. The imaging interval of the non-clean liver group was shorter than the clean liver group (3 vs 4 months, $P = 0.015$). The median intervals between the initial MRI and HCC diagnosis was 16 months (range, 9–32) in the non-clean liver group and 21 months (range, 16–35) in the clean liver group.

In 11 of 17 patients with HCC development, HCC developed at sites in which no nodules had been seen on the initial gadoxetic acid-enhanced MRI, namely de novo HCC. These HCC were found in four of 18 patients in the non-clean liver group (3-year HCC incidence rates: 22.2%; 95% CI, 4.3–51.0%) and 7 in 109 patients in the clean liver group (3-year HCC incidence rates: 6.4%; 95% CI, 1.8–11.0%). The incidence rates of de novo HCC was significantly higher in the non-clean liver group than the clean liver group ($P = 0.003$, Fig. 3). In the remaining six patients, HCC developed at the same site of the initial nodules exclusively in 18 patients of a non-clean liver group by definition, and those HCC arose among the nodules of 8 mm or more in the initial MRI study.

Risk factors for HCC development

Univariate analyses showed that the significant risk factors for HCC development included older age ($P = 0.039$), cirrhosis ($P = 0.009$), a low platelet count ($P = 0.003$), a high AFP concentration ($P = 0.006$) and a non-clean liver ($P < 0.001$). Multivariate analysis with these variables revealed that older age (hazard ratio [HR], 1.08; 95% CI, 1.01–1.16; $P = 0.024$), a low plate-

Table 1 Baseline patient characteristics

Characteristics	Total ($n = 127$)	Non-clean liver ($n = 18$)	Clean liver ($n = 109$)	<i>P</i>
Age, years	65 (30–88)	68 (46–82)	64 (30–88)	0.15
Male/female	68/59	10/8	58/51	1.00
Non-cirrhosis/cirrhosis	59/68	6/12	53/56	0.31
HBV/HCV	26/101	5/13	21/88	0.53
Platelet count ($\times 10^9/L$)	122 (30–410)	102 (46–187)	125 (30–410)	0.07
ALT (IU/L)	32 (7–206)	32 (14–95)	32 (7–206)	0.97
γ -GT (IU/L)	31 (9–305)	31 (13–258)	31 (9–305)	0.68
AFP (ng/mL)	4 (1–582)	8 (2–181)	4 (1–582)	0.19

Continuous data are shown as medians (range).

γ -GT, γ -glutamyltransferase; AFP, α -fetoprotein; ALT, alanine aminotransferase; HBV, hepatitis B virus; HCV, hepatitis C virus.

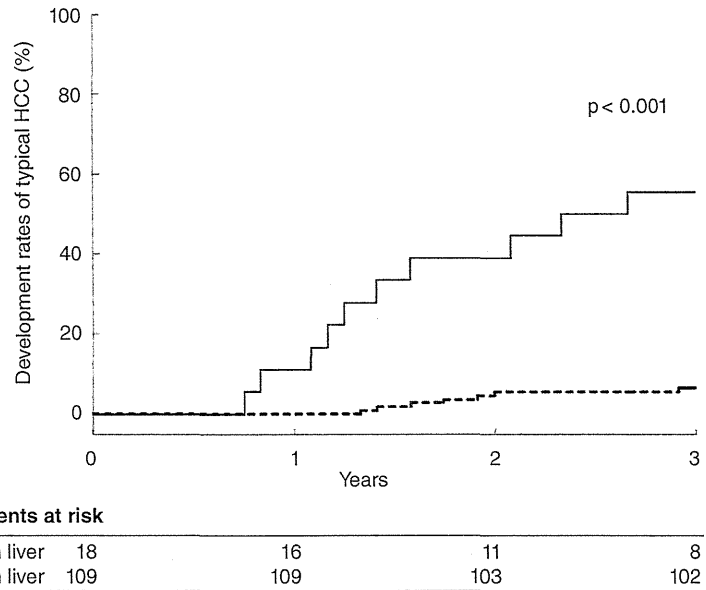


Figure 2 Cumulative incidence rates of typical hepatocellular carcinoma (HCC) development in the non-clean and clean liver groups. —, non-clean liver group ($n = 18$); ---, clean liver group ($n = 109$).

let count (HR, 1.17; 95% CI, 1.03–1.35; $P = 0.017$) and a non-clean liver (HR, 9.41; 95% CI, 3.47–25.46; $P < 0.001$) were the only independent risk factors for HCC development (Table 2).

We further assessed the effect of a non-clean liver on the risk of HCC development in subgroups of these patients (Fig. 4). We found that belonging to the non-

clean liver group was a significant risk factor in patients without HBV. Notably, this designation was particularly valuable for patients who are generally regarded as at low risk for HCC development: those without cirrhosis (HR, 37.23; 95% CI, 3.30–419.71; $P = 0.003$) and those with high platelet counts (HR, 33.42; 95% CI, 6.69–166.94; $P < 0.001$).

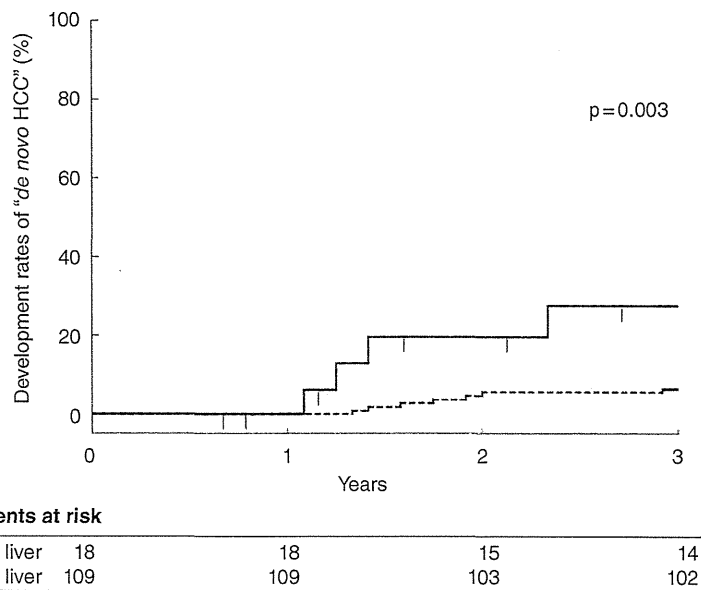


Figure 3 Cumulative incidence rates of typical hepatocellular carcinoma (HCC) at sites in which no nodules had been seen on the initial gadoxetic acid-enhanced magnetic resonance imaging, namely, "de novo HCC". —, non-clean liver group ($n = 18$); ---, clean liver group ($n = 109$).

Table 2 Variables that predict HCC development: univariate and multivariate analyses

Variables	Univariate		Multivariate	
	Hazard ratio (95% CI)	P	Hazard ratio (95% CI)	P
Male	0.56 (0.29–1.95)	0.755		
Age (per year)	1.06 (1.00–1.12)	0.039	1.08 (1.01–1.16)	0.024
Cirrhosis	14.37 (1.90–108.44)	0.009	3.54 (0.37–33.77)	0.231
HCV (vs HBV)	4.39 (0.58–33.17)	0.151		
Platelet count (per 10 ¹⁰ /L)	1.19 (1.06–1.33)	0.003	1.17 (1.03–1.35)	0.017
ALT (per IU/L)	1.00 (0.99–1.02)	0.423		
γ-GT (per IU/L)	1.00 (0.99–1.01)	0.688		
AFP >10 ng/mL	3.98 (1.47–10.77)	0.006	1.47 (0.49–4.33)	0.486
Non-clean liver	12.36 (4.68–32.61)	<0.001	9.41 (3.47–25.46)	<0.001

γ-GT, γ-glutamyltransferase; AFP, α-fetoprotein; ALT, alanine aminotransferase; CI, confidence interval; HBV, hepatitis B virus; HCC, hepatocellular carcinoma; HCV, hepatitis C virus.

DISCUSSION

THIS STUDY REVEALED presence of hypovascular hypointense liver nodules (non-clean liver) on gadoxetic acid-enhanced MRI, is a significant risk factor for subsequent development of typical HCC not only at the same sites but also at the different sites from the initial nodules. The incidence of development of typical HCC in the non-clean liver patients was more than 50% during a 3-year follow-up period, indicating that these higher risk patients should be rigorously investigated for the early detection of HCC during follow up.

In the present study, six of the 18 patients in the non-clean liver group developed typical HCC at the

same site of the initial nodules during the subsequent 3 years (11.1%/year). Most of the hypovascular hypointense nodules on gadoxetic acid-enhanced MRI are considered precursor lesions of typical HCC, such as early HCC or high-grade dysplastic nodules, on histological examination,^{13–15} while it has been reported that most hypovascular nodules exhibiting high-intensity to isointensity signals in the hepatocyte phase are benign hepatic nodules.^{14,15} Recent studies have suggested that a reduction of organic anion-transporting polypeptide 1B3 (OATP 8) transporter expression begins at the earliest stage of hepatocarcinogenesis,^{21,22} before changes in vascularity such as decreased portal flow or increased arterial flow. The progression rate of the small

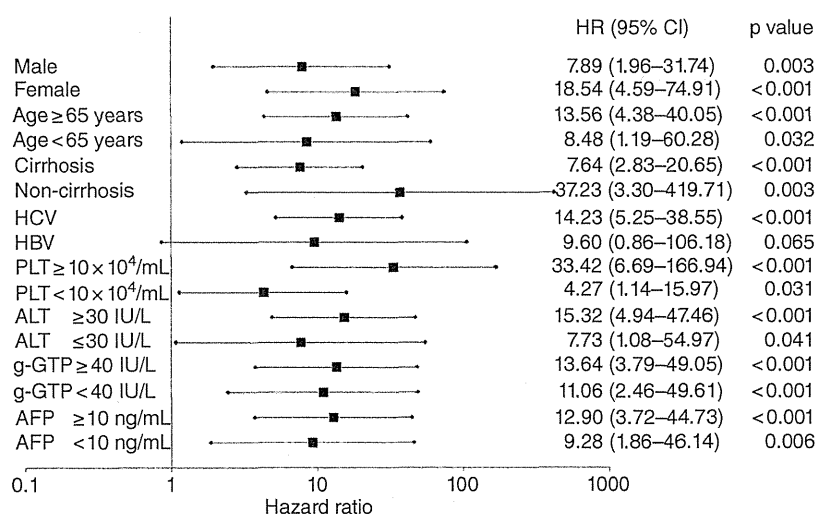


Figure 4 Stratified analyses of the non-clean liver as a risk factor for typical HCC development. AFP, α-fetoprotein; ALT, alanine aminotransferase; CI, confidence interval; g-GTP, γ-glutamyltransferase; HBV, hepatitis B virus; HCC, hepatocellular carcinoma; HCV, hepatitis C virus; HR, hazard ratio; PLT, platelets.

hypovascular hypointense nodules to typical HCC was reported as 10–17%/year,^{9,10} which is comparable to the present study. Typical HCC arose exclusively among the nodules of 8 mm or more, as in previous studies in which the larger hypovascular hypointense nodules were found to be the risk factor for progression to typical HCC in the initial MRI study.^{9,10}

Hyperintensity on T2WI¹² or diffusion-weighted images (DWI)¹¹ also was reported to be useful for prediction of typical HCC progress in hypovascular hypointense nodules. In our patients, none of the nodules in the non-clean liver group showed hyperintensity on T2WI, suggesting that the hepatocyte phase is more sensitive for detecting the early stage of hepatocarcinogenesis.¹⁵ DWI were not evaluated in this study because this usually detects pathologically advanced HCC of larger size or with hypervascularity.²³ Thus, it is reasonable that the hepatocyte phase can effectively recognize the earliest stage of HCC development without T2WI or DWI.

In 11 of 17 patients, typical HCC developed at sites other than the initially detected hypovascular hypointense nodules. As shown in Figure 3, the incidence rates of such HCC in the non-clean liver group was significantly higher than in the clean liver group ($P=0.003$), indicating that a non-clean liver itself is a risk factor for HCC development, apart from the detectable hypovascular hypointense nodules. In addition, in four patients with nodules even below 8 mm, two developed HCC at different sites from the initial nodules during follow up (data not shown). Taken together, a non-clean liver has the higher potential for hepatocarcinogenesis or for undetectable precursor lesions. The non-clean liver may reflect more advanced genetic or epigenetic changes in the background hepatocytes, however, the detailed biological mechanism is not clear in this study.

Non-clean liver was an independent risk factor for the development of typical HCC, apart from well-documented risk factors (Table 2), such as cirrhosis,²⁴ ALT,²⁵ γ -GT,²⁶ age and AFP.²⁷ A non-clean liver is a significant risk for HCC development also for those without cirrhosis or with high platelet counts (Fig. 4). This means patients at increased risk of HCC development can be discerned as having a non-clean liver even among low-risk subgroups.

Conversely, patients without such nodules (clean liver group) showed a significantly lower risk of developing typical HCC than those with non-clean livers (0.0% vs 11.1% at 1 year, 6.8% vs 55.5% at 3 years of follow up; $P<0.001$), suggesting that gadoteric acid-enhanced

MRI could detect precursor lesions sensitively enough to rule out immediate (within 1 year) development of typical HCC. Although seven patients in the clean liver group developed typical HCC only after 1 year, these patients had other risk factors for HCC development, including lower platelet counts, implying more advanced liver cirrhosis or high AFP (data not shown). Such HCC may arise from precursor lesions that cannot be visualized by current imaging techniques.

This study is a retrospective study and has some limitations. We included patients with HBV and HCV together, because gadoteric acid-enhanced MRI findings or HCC development do not differ between these two groups and HBV or HCV infection is not an independent risk factor for typical HCC development. However, the number of HBV patients was too small ($n=26$) to statistically confirm the current result when limited to HBV patients only. Prospective studies with larger numbers of patients who have uniform liver disease etiologies and imaging intervals are needed to verify our findings in different settings. Although the imaging interval of the non-clean liver group was shorter than the clean liver group (3 vs 4 months; $P=0.015$), the median intervals between the initial MRI and HCC diagnosis was 16 months in the non-clean liver group and 21 months in the clean liver group. They are short enough for cumulative detection of HCC development for 3 years and it is assumed that there was little influence on the conclusions.

In conclusion, patients with chronic viral liver disease are at high risk for developing typical HCC at any sites of the liver if they have hypovascular hypointense nodules on gadoteric acid-enhanced MRI. These patients should be closely followed up for developing typical HCC not only at the same site but also at different sites from the initial nodule.

REFERENCES

- 1 Ichikawa T, Saito K, Yoshioka N *et al.* Detection and characterization of focal liver lesions: a Japanese phase III, multicenter comparison between gadoteric acid disodium-enhanced magnetic resonance imaging and contrast-enhanced computed tomography predominantly in patients with hepatocellular carcinoma and chronic liver disease. *Invest Radiol* 2010; 45: 133–41.
- 2 Halavaara J, Breuer J, Ayuso C *et al.* Liver tumor characterization: comparison between liver-specific gadoteric acid disodium-enhanced MRI and biphasic CT – a multicenter trial. *J Comput Assist Tomogr* 2006; 30: 345–54.
- 3 Hamm B, Staks T, Muhler A *et al.* Phase I clinical evaluation of Gd-EOB-DTPA as a hepatobiliary MR contrast

- agent: safety, pharmacokinetics, and MR imaging. *Radiology* 1995; 195: 785–92.
- 4 Hammerstingl R, Huppertz A, Breuer J *et al.* European EOB-study group. Diagnostic efficacy of gadoxetic acid (Primovist)-enhanced MRI and spiral CT for a therapeutic strategy: comparison with intraoperative and histopathologic findings in focal liver lesions. *Eur Radiol* 2008; 18: 457–67.
 - 5 Huppertz A, Balzer T, Blakeborough A *et al.* European EOB Study Group. Improved detection of focal liver lesions at MR imaging: multicenter comparison of gadoxetic acid-enhanced MR images with intraoperative findings. *Radiology* 2004; 230 (1): 266–75.
 - 6 Di Martino M, Marin D, Guerrisi A *et al.* Intraindividual comparison of gadoxetate disodium-enhanced MR imaging and 64-section multidetector CT in the detection of hepatocellular carcinoma in patients with cirrhosis. *Radiology* 2010; 256: 806–16.
 - 7 Inoue T, Kudo M, Komuta M *et al.* Assessment of Gd-EOB-DTPA-enhanced MRI for HCC and dysplastic nodules and comparison of detection sensitivity versus MDCT. *J Gastroenterol* 2012; 47: 1036–47.
 - 8 Golfieri R, Renzulli M, Lucidi V, Corcioni B, Trevisani F, Bolondi L. Contribution of the hepatobiliary phase of Gd-EOB-DTPA-enhanced MRI to dynamic MRI in the detection of hypovascular small (≤ 2 cm) HCC in cirrhosis. *Eur Radiol* 2011; 21: 1233–42.
 - 9 Kumada T, Toyoda H, Tada T *et al.* Evolution of hypointense hepatocellular nodules observed only in the hepatobiliary phase of gadoxetate disodium-enhanced MRI. *AJR Am J Roentgenol* 2011; 197 (1): 58–63.
 - 10 Motosugi U, Ichikawa T, Sano K *et al.* Outcome of hypovascular hepatic nodules revealing no gadoxetic acid uptake in patients with chronic liver disease. *J Magn Reson Imaging* 2011; 34 (1): 88–94.
 - 11 Kim YK, Lee WJ, Park MJ, Kim SH, Rhim H, Choi D. Hypovascular hypointense nodules on hepatobiliary phase gadoxetic acid-enhanced MR images in patients with cirrhosis: potential of DW imaging in predicting progression to hypervascular HCC. *Radiology* 2012; 265 (1): 104–14.
 - 12 Hyodo T, Murakami T, Imai Y *et al.* Hypovascular nodules in patients with chronic liver disease: risk factors for development of hypervascular hepatocellular carcinoma. *Radiology* 2013; 266: 480–90.
 - 13 Bartolozzi C, Battaglia V, Bargellini I *et al.* Contrast-enhanced magnetic resonance imaging of 102 nodules in cirrhosis: correlation with histological findings on explanted livers. *Abdom Imaging* 2013; 38: 290–6.
 - 14 Golfieri R, Grazioli L, Orlando E *et al.* Which is the best MRI marker of malignancy for atypical cirrhotic nodules: hypointensity in hepatobiliary phase alone or combined with other features? Classification after Gd-EOB-DTPA administration. *J Magn Reson Imaging* 2012; 36: 648–57.
 - 15 Sano K, Ichikawa T, Motosugi U *et al.* Imaging study of early hepatocellular carcinoma: usefulness of gadoxetic acid-enhanced MR imaging. *Radiology* 2011; 261: 834–44.
 - 16 Motosugi U. Hypovascular hypointense nodules on hepatocyte phase gadoxetic acid-enhanced MR images: too early or too progressed to determine hypervascularity. *Radiology* 2013; 267 (1): 317–8.
 - 17 Asayama Y, Yoshimitsu K, Nishihara Y *et al.* Arterial blood supply of hepatocellular carcinoma and histologic grading: radiologic-pathologic correlation. *AJR Am J Roentgenol* 2008; 190 (1): W28–34.
 - 18 Motosugi U, Ichikawa T, Sou H *et al.* Liver parenchymal enhancement of hepatocyte-phase images in Gd-EOB-DTPA-enhanced MR imaging: which biological markers of the liver function affect the enhancement? *J Magn Reson Imaging* 2009; 30: 1042–6.
 - 19 Bruix J, Sherman M, American Association for the Study of Liver Diseases. Management of hepatocellular carcinoma: an update. *Hepatology* 2011; 53: 1020–2.
 - 20 Motosugi U, Ichikawa T, Araki T. Rules, roles, and room for discussion in gadoxetic acid-enhanced magnetic resonance liver imaging: current knowledge and future challenges. *Magnetic Resonance in Medical Sciences*. 2013; 12: 161–75.
 - 21 Kitao A, Zen Y, Matsui O *et al.* Hepatocellular carcinoma: signal intensity at gadoxetic acid-enhanced MR imaging – correlation with molecular transporters and histopathologic features. *Radiology* 2010; 256: 817–26.
 - 22 Narita M, Hatano E, Arizono S *et al.* Expression of OATP1B3 determines uptake of Gd-EOB-DTPA in hepatocellular carcinoma. *J Gastroenterol* 2009; 44: 793–8.
 - 23 Nasu K, Kuroki Y, Tsukamoto T, Nakajima H, Mori K, Minami M. Diffusion-weighted imaging of surgically resected hepatocellular carcinoma: imaging characteristics and relationship among signal intensity, apparent diffusion coefficient, and histopathologic grade. *American Journal of Roentgenology* 2009; 193: 438–44.
 - 24 Degos F, Christidis C, Ganne-Carrie N *et al.* Hepatitis C virus related cirrhosis: time to occurrence of hepatocellular carcinoma and death. *Gut* 2000; 47 (1): 131–6.
 - 25 Tarao K, Rino Y, Ohkawa S *et al.* Association between high serum alanine aminotransferase levels and more rapid development and higher rates of incidence of hepatocellular carcinoma in patients with hepatitis C virus-associated cirrhosis. *Cancer* 1999; 86: 589–95.
 - 26 Ikeda K, Saitoh S, Suzuki Y *et al.* Disease progression and hepatocellular carcinogenesis in patients with chronic viral hepatitis: a prospective observation of 2215 patients. *J Hepatol* 1998; 28: 930–8.
 - 27 Ikeda K, Saitoh S, Koida I *et al.* A multivariate analysis of risk factors for hepatocellular carcinogenesis: a prospective observation of 795 patients with viral and alcoholic cirrhosis. *Hepatology* 1993; 18 (1): 47–53.

Original Article

Prospective comparison of real-time tissue elastography and serum fibrosis markers for the estimation of liver fibrosis in chronic hepatitis C patients

Nobuharu Tamaki,¹ Masayuki Kurosaki,¹ Shuya Matsuda,¹ Toru Nakata,¹ Masaru Muraoka,¹ Yuichiro Suzuki,¹ Yutaka Yasui,¹ Shoko Suzuki,¹ Takanori Hosokawa,¹ Takashi Nishimura,¹ Ken Ueda,¹ Kaoru Tsuchiya,¹ Hiroyuki Nakanishi,¹ Jun Itakura,¹ Yuka Takahashi,¹ Kotaro Matsunaga,^{2,4} Kazuhiro Taki,² Yasuhiro Asahina³ and Namiki Izumi¹

Divisions of ¹Gastroenterology and Hepatology and ²Pathology, Musashino Red Cross Hospital, ³Division of Gastroenterology and Hepatology, Tokyo Medical and Dental University, Tokyo and ⁴Division of Gastroenterology and Hepatology, St Marianna University School of Medicine, Kanagawa, Japan

Aim: Real-time tissue elastography (RTE) is a non-invasive method for the measurement of tissue elasticity using ultrasonography. Liver fibrosis (LF) index is a quantitative method for evaluation of liver fibrosis calculated by RTE image features. This study aimed to investigate the significance of LF index for predicting liver fibrosis in chronic hepatitis C patients.

Methods: In this prospective study, 115 patients with chronic hepatitis C who underwent liver biopsy were included, and the diagnostic accuracy of LF index and serum fibrosis markers was evaluated.

Results: RTE imaging was successfully performed on all patients. Median LF index in patients with F0–1, F2, F3 and F4 were 2.61, 3.07, 3.54 and 4.25, respectively, demonstrating a stepwise increase with liver fibrosis progression ($P < 0.001$). LF index (odds ratio [OR] = 5.3, 95% confidence interval [CI] = 2.2–13.0) and platelet count (OR = 0.78, 95% CI = 0.68–

0.89) were independently associated with the presence of advanced fibrosis (F3–4). Further, LF index was independently associated with the presence of minimal fibrosis (F0–1) (OR = 0.25, 95% CI = 0.11–0.55). The area under the receiver–operator curve (AUROC) of LF index for predicting advanced fibrosis (0.84) was superior to platelets (0.82), FIB-4 index (0.80) and aspartate aminotransferase/platelet ratio index (APRI) (0.76). AUROC of LF index (0.81) was superior to platelets (0.73), FIB-4 index (0.79) and APRI (0.78) in predicting minimal fibrosis.

Conclusion: LF index calculated by RTE is useful for predicting liver fibrosis, and diagnostic accuracy of LF index is superior to serum fibrosis markers.

Key words: chronic hepatitis C, fibrosis, liver fibrosis index, real-time tissue elastography

INTRODUCTION

AN ADVANCED STAGE of liver fibrosis in chronic hepatitis C (CHC) is associated with hepatocellular carcinoma development and complications such as

esophageal variceal bleeding and liver failure.^{1,2} Therefore, accurate evaluation of the stage of liver fibrosis is most important in clinical practice. Liver biopsy is considered to be the golden standard for diagnosis of liver fibrosis.^{3–5} However, this method may be inaccurate because of sampling errors and interobserver variations.^{6,7}

Improvements in a variety of non-invasive methods for evaluating liver fibrosis have recently emerged as alternatives to liver biopsy. Liver fibrosis was reportedly predicted by measurement of liver stiffness using transient elastography^{8,9} and acoustic radiation force impulse (ARFI).^{10,11} As assessed by blood laboratory tests, the aspartate aminotransferase (AST)/alanine

Correspondence: Dr Namiki Izumi, Department of Gastroenterology and Hepatology, Musashino Red Cross Hospital, 1-26-1 Kyonan-cho, Musashino-shi, Tokyo 180-8610, Japan. Email: nizumi@musashino.jrc.or.jp

Conflict of interest: The authors who have taken part in this study declare that they do not have anything to disclose regarding funding or conflict of interest with respect to this manuscript. Received 28 January 2013; revision 20 May 2013; accepted 29 May 2013.

aminotransferase (ALT) ratio,¹² AST/platelet ratio index (APRI),^{13,14} and FIB-4 index^{15,16} have been reported to be useful for the prediction of liver fibrosis. We previously reported that the FIB-4 index is useful for the prediction of liver fibrosis progression.¹⁷

Real-time tissue elastography (RTE) is a non-invasive method for the measurement of tissue elasticity using ultrasonography.¹⁸ RTE calculates the relative hardness of tissue from the degree of tissue distortion and displays this information as a color image. RTE was recently reported to be useful for predicting liver fibrosis.^{19,20} To increase the objectivity of the evaluation, an image analysis method to evaluate the strain image features and a new algorithm to deliver an index were proposed. Liver fibrosis (LF) index is a quantitative method for evaluation of liver fibrosis that is calculated by nine RTE image features, and the significance of LF index for predicting liver fibrosis has been reported.^{21,22}

In the present study, we prospectively investigated the significance of LF index calculated by RTE for the prediction of liver fibrosis in CHC patients. Further, diagnostic accuracy for liver fibrosis was compared between LF index and serum fibrosis markers.

METHODS

Patients

A TOTAL OF 127 consecutive patients with CHC were prospectively investigated. All patients underwent liver biopsy at Musashino Red Cross Hospital between February 2011 and November 2012. Exclusion criteria comprised the following: (i) co-infection with hepatitis B virus ($n = 1$); (ii) co-infection with HIV ($n = 1$); (iii) history of autoimmune hepatitis or primary biliary cirrhosis ($n = 3$); (iv) alcohol abuse (intake of alcohol equivalent to pure alcohol ≥ 40 g/day) ($n = 0$); (v) portal tracts of biopsy sample of less than five ($n = 7$); and (vi) presence of serious heart disease ($n = 0$). After exclusion, 115 patients were enrolled in this study. Written informed consent was obtained from each patient and the study protocol conformed to the ethical guidelines of the Declaration of Helsinki and was approved by the institutional ethics review committees (application no. 24007).

Histological evaluation

Liver biopsy specimens were laparoscopically obtained using 13-G needles ($n = 93$). When laparoscopy was not conducted due to a history of upper abdominal surgery, percutaneous ultrasound-guided liver biopsy

was performed using 15-G needles ($n = 22$). Specimens were fixed, paraffin-embedded, and stained with hematoxylin–eosin and Masson-trichrome. A biopsy sample with minimum portal tracts of five was required for diagnosis. All liver biopsy samples were independently evaluated by two senior pathologists who were blinded to the clinical data. Fibrosis staging was categorized according to the METAVIR score:²³ F0, no fibrosis; F1, portal fibrosis without septa; F2, portal fibrosis with few septa; F3, numerous septa without cirrhosis; and F4, cirrhosis. Activity of necroinflammation was graded on a scale of 0–3: A0, no activity; A1, mild activity; A2, moderate activity; and A3, severe activity. Percentage of steatosis was quantified by determining the average proportion of hepatocytes affected by steatosis and graded on a scale of 0–3: grade 0, no steatosis; grade 1, 1–33%; grade 2, 34–66%; and grade 3, 67% and over.

Clinical and biological data

The age and sex of the patients were recorded. Serum samples were collected within 1 day prior to liver biopsy and the following variables were obtained through serum sample analysis: AST, ALT and platelet count. FIB-4 index and APRI were calculated according to the published formula appropriate to each measure.^{13,15}

RTE and LF index

Real-time tissue elastography was performed using HI VISION Preirus (Hitachi Aloka Medical, Tokyo, Japan) and the EUP-L52 linear probe (3–7 MHz; Hitachi Aloka Medical) within 3 days of liver biopsy. RTE was performed on the right lobe of the liver through the intercostal space. An RTE image was induced by heartbeats. Five RTE images were collected for each patient and analyzed to calculate nine image features. RTE method and the equation that calculates LF index using nine image features has been previously detailed.²² Results are expressed as mean LF index of all measurements. Two hepatologists (N. T. and K. Tsuchiya, with 8 and 16 years of experience, respectively) performed RTE. In 32 patients with CHC, LF index was measured independently by two examiners. The correlation coefficient of LF index between two examiners was 0.85 ($P \leq 0.001$).

Statistical analysis

Correlations between LF index and histological fibrosis stage were analyzed using Spearman's rank correlation coefficients. Categorical variables were compared using Fisher's exact test, and continuous variables were compared using Mann–Whitney *U*-test. $P < 0.05$ was considered statistically significant. Logistic regression was

used for multivariate analysis. Receiver–operator curves (ROC) were constructed, and the area under the ROC (AUROC) was calculated. Optimal cut-off values were selected, to maximize sensitivity, specificity and diagnostic accuracy. Sensitivity, specificity, positive predictive value (PPV) and negative predictive value (NPV) were calculated by using cut-offs obtained by ROC. SPSS software ver. 15.0 (SPSS, Chicago, IL, USA) was used for analyses.

RESULTS

Patient characteristics

THE CHARACTERISTICS OF all 115 patients are listed in Table 1. F0–1 was diagnosed in 52 cases (45%), F2 in 31 (27%), F3 in 20 (17%) and F4 in 12 (11%). Mean values of LF index of F0 (2.62) and F1 (2.60) were not significantly different ($P = 0.9$), and only six patients with F0 were included in this study. Therefore, patients with F0 and F1 were integrated for the analysis. RTE imaging was successfully performed in all patients, and LF index was calculated.

Relationship between histological findings and LF index by RTE

The median value of LF index compared with the METAVIR fibrosis stage is shown in Figure 1. Median LF

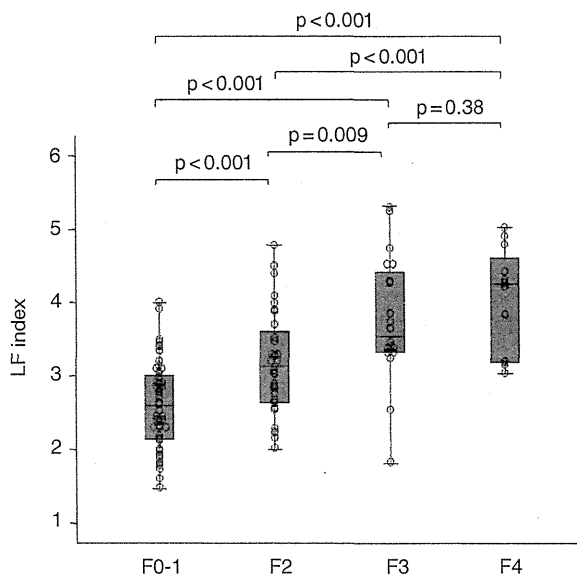


Figure 1 Correlation between liver fibrosis (LF) index calculated by real-time tissue elastography and fibrosis stage. Box plot of the LF index is shown according to each fibrosis stage. The bottom and top of each box represent the 25th and 75th percentiles, giving the interquartile range. The line through the box indicates the median value, and error bar indicates minimum and maximum non-extreme values.

Table 1 Patient characteristics

Characteristics	Patients (n = 115)
Female/male	68/47
Age (years)	57.9 ± 10.9
AST (IU/L)	55.7 ± 44.9
ALT (IU/L)	63.2 ± 56.3
Platelet counts (×10 ⁹ /L)	162 ± 53
Portal tracts of biopsy samples	12.6 ± 5.0
Fibrosis stage	
F0–1 (%)	51 (44)
F2 (%)	32 (28)
F3 (%)	20 (17)
F4 (%)	12 (11)
Histological activity	
A0 (%)	0 (0)
A1 (%)	75 (65)
A2 (%)	34 (30)
A3 (%)	6 (5)
Steatosis grade	
Grade 0 (%)	65 (57)
Grade 1 (%)	47 (41)
Grade 2 (%)	3 (2)
Grade 3 (%)	0 (0)

ALT, alanine aminotransferase; AST, aspartate aminotransferase.

index in patients with F0–1, F2, F3 and F4 were 2.61, 3.07, 3.54 and 4.25, respectively, demonstrating a step-wise increase with liver fibrosis progression ($P < 0.001$). LF index of each fibrosis stage significantly differed from each other (F0–1 vs F2, $P < 0.001$; F0–1 vs F3, $P < 0.001$; F0–1 vs F4, $P < 0.001$; F2 vs F3, $P = 0.009$; F2 vs F4, $P = 0.001$). On the other hand, mean values of LF index in patients with steatosis grade 0, 1 and 2 were 2.99, 3.29 and 2.60, respectively, demonstrating no significant correlation (Fig. 2a). LF index was compared with steatosis grade for each fibrosis stage. LF index was not significantly different between patients with steatosis and without steatosis (Fig. 2b).

Liver fibrosis index was compared with histological activity. A significant correlation existed between histological activity and fibrosis stage. Therefore, the relationship between LF index and histological activity was examined by each fibrosis stage. In patients with F0–1, the mean LF index of A1, A2 and A3 was 2.60, 2.58 and 2.40, respectively, demonstrating no significant correlation. Similarly, in patients with F2, F3 and F4, there was no significant correlation between LF index and histological activity (Fig. 3).

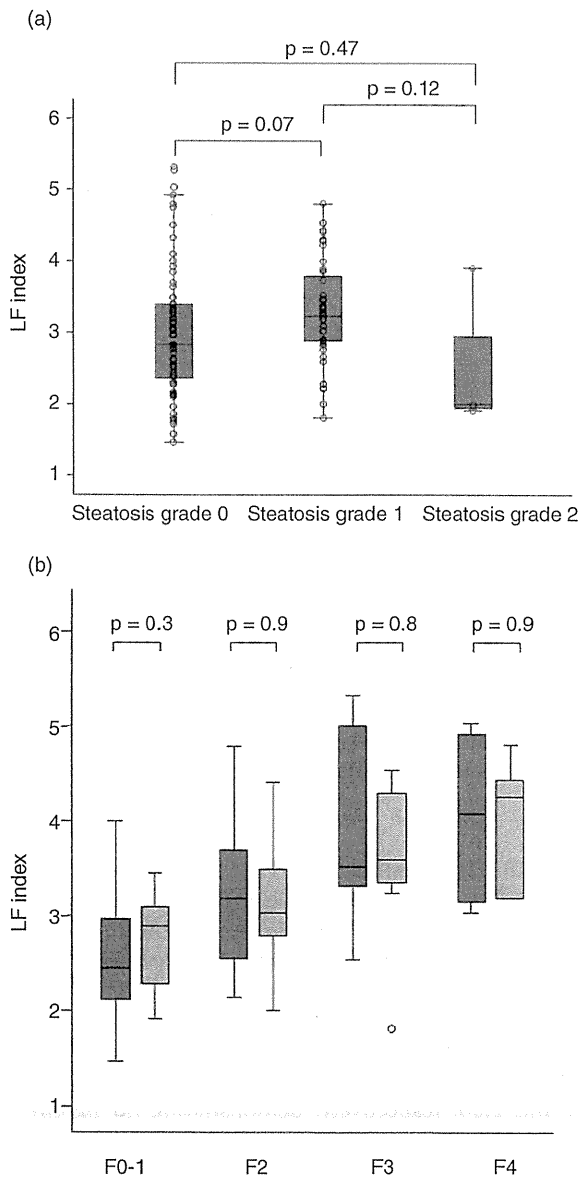


Figure 2 (a) Correlation between liver fibrosis (LF) index and steatosis grade. Box plot of the LF index is shown according to each steatosis grade. The bottom and top of each box represent the 25th and 75th percentiles, giving the interquartile range. The line through the box indicates the median value, and error bar indicates minimum and maximum non-extreme values. (b) Box plot of LF index for each fibrosis stage in relation to degree of steatosis grade. The bottom and top of each box represent the 25th and 75th percentiles, giving the interquartile range. The line through the box indicates the median value, and error bar indicates minimum and maximum non-extreme values. Dark grey bar chart indicates steatosis grade 0. Light grey bar chart indicates steatosis grade 1–2.

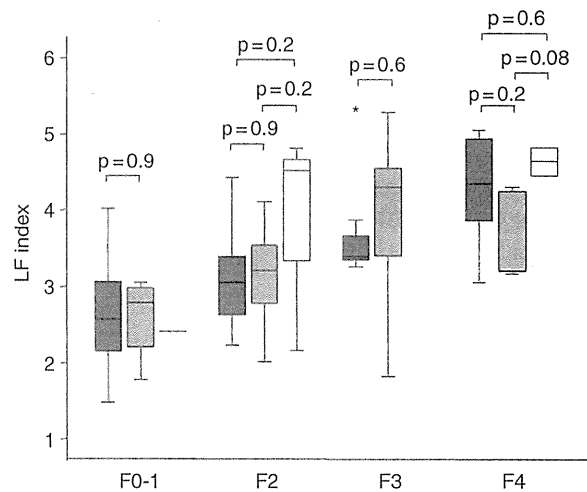


Figure 3 Box plot of liver fibrosis (LF) index for each fibrosis stage in relation to degree of necroinflammatory activity. The bottom and top of each box represent the 25th and 75th percentiles, giving the interquartile range. The line through the box indicates the median value, and error bar indicates minimum and maximum non-extreme values. Dark grey bar chart indicates activity grade 1. Light grey bar chart indicates activity grade 2. White bar chart indicates activity grade 3.

Comparison of variables associated with the presence of advanced fibrosis (F3–4) by univariate and multivariate analysis

Variables associated with the presence of advanced fibrosis (F3–4) were assessed by univariate and multivariate analysis (Table 2). The variables of age ($P = 0.03$) and LF index ($P < 0.001$) were significantly higher, and the variable of platelets ($P < 0.001$) was significantly lower in patients with advanced fibrosis than in patients with F0–2. Multivariate analysis showed that LF index (odds ratio [OR] = 5.3, 95% confidence interval [CI] = 2.2–13.0) and platelets (OR = 0.78, 95% CI = 0.68–0.89) were independently associated with the presence of advanced fibrosis.

Comparison of variables associated with the presence of minimal fibrosis (F0–1) by univariate and multivariate analysis

Variables associated with the presence of minimal fibrosis (F0–1) were assessed by univariate and multivariate analysis (Table 3). The variables of age ($P < 0.001$), AST ($P = 0.02$) and LF index ($P < 0.001$) were significantly lower, and the variable of platelets ($P < 0.001$) was significantly higher in F0–1 patients than F2–4 patients.

Table 2 Variables associated with the presence of advanced fibrosis (F3–4) by univariate and multivariate analysis

	F0–2 (n = 83)	F3–4 (n = 32)	P-value (Univariate)	Odds ratio (95% CI) (Multivariate)
Age (years)	56.6 ± 10.9	61.3 ± 10.4	0.03	
Sex (female/male)	51/32	17/15	0.41	
AST (IU/L)	52.3 ± 43.3	64.4 ± 48.3	0.19	
ALT (IU/L)	62.9 ± 60.6	63.9 ± 44.2	0.93	
Platelets (×10 ⁹ /L)	179 ± 47	117 ± 42	<0.001	0.78 (0.68–0.89)
LF index	2.81 ± 0.69	3.86 ± 0.81	<0.001	5.30 (2.16–13.0)

ALT, alanine aminotransferase; AST, aspartate aminotransferase; CI, confidence interval; LF, liver fibrosis.

Multivariate analysis showed that LF index was independently associated with the presence of minimal fibrosis (OR = 0.25, 95% CI = 0.11–0.55).

Diagnostic accuracy of RTE and serum fibrosis markers

Receiver–operator curves of LF index, platelets, FIB-4 index and APRI for predicting advanced fibrosis (F3–4), and minimal fibrosis (F0–1) were plotted, as shown in Figure 4. AUROC of LF index for predicting advanced fibrosis (0.84) was superior to platelets (0.82), FIB-4 index (0.80) and APRI (0.76). Similarly, for predicting minimal fibrosis, AUROC of LF index (0.81) was superior to platelets (0.73), FIB-4 index (0.79) and APRI (0.78). The corresponding sensitivities, specificities, PPV and NPV are detailed in Table 4.

DISCUSSION

IMPROVEMENTS IN VARIOUS methods for prediction of liver fibrosis have recently emerged as alternatives to liver biopsy. RTE is a non-invasive method for the measurement of tissue elasticity using ultrasonography. The utility of RTE for evaluating liver fibrosis is reported in a few studies.^{18–22} However, for utilizing LF

index, one of the equations used to calculate tissue elasticity by RTE is still unclear. The aim of this study was to investigate the significance of LF index for the prediction of liver fibrosis in CHC patients.

In this prospective study, we found that LF index is a useful predictive factor for diagnosis of the fibrosis stage in CHC patients. Increase in LF index significantly correlated with progression of the fibrosis stage and LF index was able to predict the presence of advanced fibrosis and minimal fibrosis. Previous studies reported the utility of LF index for prediction of the liver fibrosis stage.^{21,22} In this study, LF index differed significantly between patients with F0–1 and F2; thus, LF index was especially useful for prediction of minimal fibrosis. This may be due to a sufficient number of patients with F0–1 and F2 included in the present study. This is an advantage of LF index because other quantitative methods by RTE could not discriminate patients with F0–1 and F2.^{19,20} On the other hand, there is a possibility that a similar result may be obtained for differentiation of F3 and F4 if a large number of patients with advanced fibrosis was included.

Previous studies did not compare the diagnostic accuracy of LF index and serum fibrosis markers. We revealed that LF index performed better than serum fibrosis

Table 3 Variables associated with the presence of minimal fibrosis (F0–1) by univariate and multivariate analysis

	F0–1 (n = 51)	F2–4 (n = 64)	P-value (Univariate)	Odds ratio (95% CI) (Multivariate)
Age (years)	54.0 ± 11.9	61.0 ± 9.0	<0.001	
Sex (female/male)	31/20	37/27	0.74	
AST (IU/L)	44.5 ± 42.6	64.6 ± 44.9	0.02	
ALT (IU/L)	53.0 ± 56.3	71.3 ± 55.5	0.08	
Platelets (×10 ⁹ /L)	186 ± 47	142 ± 50	<0.001	
LF index	2.60 ± 0.59	3.51 ± 0.84	<0.001	0.25 (0.11–0.55)

ALT, alanine aminotransferase; AST, aspartate aminotransferase; CI, confidence interval; LF, liver fibrosis.

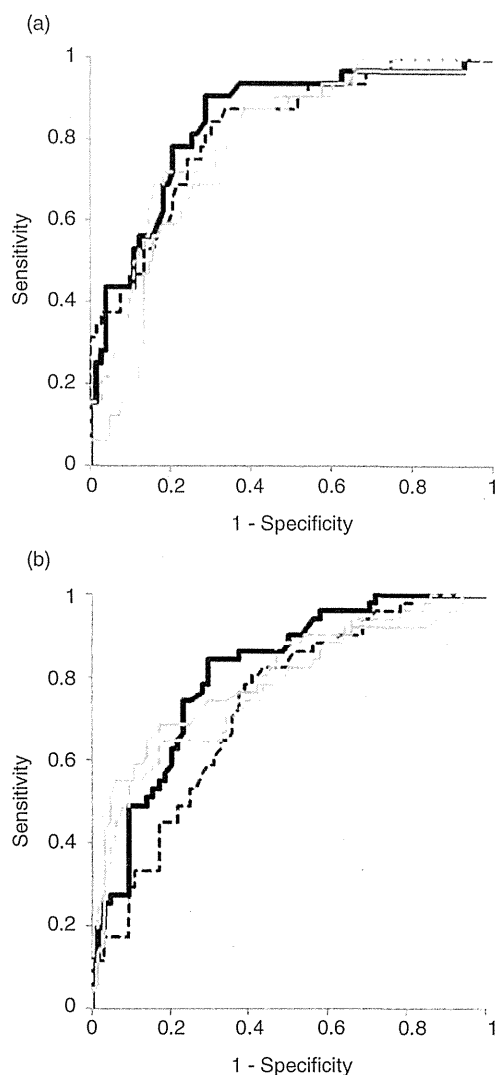


Figure 4 Receiver–operator curves (ROC) of liver fibrosis (LF) index and serum fibrosis markers. (a) ROC for diagnosis of significant fibrosis (F3–4). (b) ROC for diagnosis of minimal fibrosis (F0–1). —, LF index; ---, platelets; ···, aspartate aminotransferase-to-platelet ratio index; - · - ·, FIB-4 index.

markers based on blood laboratory tests for predicting liver fibrosis.

Transient elastography has been most commonly used to measure liver stiffness and is established in clinical practice to evaluate liver fibrosis.^{8,9} RTE exhibits some advantages compared with transient elastography. In this study, RTE imaging was successfully performed in all patients, and LF index was calculated. Although transient elastography has high diagnostic

capabilities when it comes to liver fibrosis, measurements are sometimes impossible in patients with severe obesity and ascites.²⁴ Reproducibility of transient elastography was reportedly lower in patients with steatosis, inflammation, increased body mass index and lower degrees of liver fibrosis.^{25–27} On the other hand, LF index is measured by ultrasound guidance that facilitates the identification of a suitable location for elastographic measurement, thereby resulting in a higher number of patients with valid results.

Unlike transient elastography, another advantage of LF index is that the results are not influenced by the presence of inflammation and steatosis. It was reported that LF index is not useful in patients with steatosis.²² However, LF index was not significantly different between patients with and without steatosis in the present study even after stratification by fibrosis stage. Thus, LF index was useful for prediction of fibrosis in CHC patients regardless of steatosis. Because LF index of each activity grade and steatosis grade did not differ from each other, estimation of liver fibrosis by LF index demonstrated higher reproducibility than transient elastography.

In previously reports, diagnostic accuracy of liver fibrosis using RTE was inferior to transient elastography,²⁸ however, other studies have reported contrasting results.¹⁹ The reason for this variability is probably because RTE technology and the equations used to calculate tissue elasticity are rapidly changing. The utility of elastic ratio, another RTE method for evaluation of liver fibrosis, was reported.²⁰ The elastic ratio is the ratio between the tissue compressibility of the liver and that of the intrahepatic small vessel. The AUROC of elastic ratio for predicting advanced fibrosis was 0.94 and was superior to LF index. Further, ARFI and real-time shear wave elastography were reported to have a high diagnostic accuracy of liver fibrosis.^{10,11,29} There are currently no studies that directly compare LF index and those methods for diagnostic value of liver fibrosis. Therefore, further studies are needed to fully explore the potential of RTE, especially with regard to LF index.

Our study had several limitations. The number of patients with advanced fibrosis was small. The potential of LF index to differentiate patients with F3 and F4 needs to be explored with a large number of patients. Further, validation study is needed to evaluate the diagnostic accuracy of fibrosis stage, especially in comparison with other modalities.

In conclusion, LF index calculated by RTE is useful for predicting liver fibrosis, and diagnostic accuracy of LF index is superior to that of serum fibrosis markers.

Table 4 Diagnostic performance of LF index and serum fibrosis markers

	F0–2 vs F3–4					F0–1 vs F2–4				
	AUROC	Sensitivity (%)	Specificity (%)	PPV (%)	NPV (%)	AUROC	Sensitivity (%)	Specificity (%)	PPV (%)	NPV (%)
LF index	0.84	90.6	71.1	54.7	95.2	0.81	84.3	70.3	69.4	84.9
Platelets	0.82	87.5	66.3	50.0	93.2	0.73	80.4	59.4	61.2	79.2
FIB-4 index	0.80	71.9	81.9	60.5	88.3	0.79	54.9	90.6	82.3	71.6
APRI	0.76	87.5	61.4	46.7	92.7	0.78	64.7	85.9	78.6	75.3

APRI, aspartate aminotransferase/platelet ratio index; AUROC, area under the receiver–operator curve; NPV, negative predictive value; PPV, positive predictive value.

ACKNOWLEDGMENT

THIS STUDY WAS supported by a Grant-in-Aid from Ministry of Health, Labor, and Welfare, Japan.

REFERENCES

- Serfaty L, Aumaitre H, Chazouilleres O *et al.* Determinants of outcome of compensated hepatitis C virus-related cirrhosis. *Hepatology* 1998; 27: 1435–40.
- Benvegnu L, Gios M, Boccato S, Alberti A. Natural history of compensated viral cirrhosis: a prospective study on the incidence and hierarchy of major complications. *Gut* 2004; 53: 744–9.
- Dienstag JL. The role of liver biopsy in chronic hepatitis C. *Hepatology* 2002; 36: S152–60.
- Gebo KA, Herlong HF, Torbenson MS *et al.* Role of liver biopsy in management of chronic hepatitis C: a systematic review. *Hepatology* 2002; 36: S161–72.
- Namiki I, Nishiguchi S, Hino K *et al.* Management of hepatitis C; Report of the Consensus Meeting at the 45th Annual Meeting of the Japan Society of Hepatology (2009). *Hepatol Res* 2010; 40: 347–68.
- Bedossa P, Dargere D, Paradis V. Sampling variability of liver fibrosis in chronic hepatitis C. *Hepatology* 2003; 38: 1449–57.
- Intraobserver and interobserver variations in liver biopsy interpretation in patients with chronic hepatitis C. The French METAVIR Cooperative Study Group. *Hepatology* 1994; 20: 15–20.
- Sandrin L, Fourquet B, Hasquenoph JM *et al.* Transient elastography: a new noninvasive method for assessment of hepatic fibrosis. *Ultrasound Med Biol* 2003; 29: 1705–13.
- Friedrich-Rust M, Ong MF, Martens S *et al.* Performance of transient elastography for the staging of liver fibrosis: a meta-analysis. *Gastroenterology* 2008; 134: 960–74.
- Friedrich-Rust M, Wunder K, Kriener S *et al.* Liver fibrosis in viral hepatitis: noninvasive assessment with acoustic radiation force impulse imaging versus transient elastography. *Radiology* 2009; 252: 595–604.
- Palmeri ML, Wang MH, Rouze NC *et al.* Noninvasive evaluation of hepatic fibrosis using acoustic radiation force-based shear stiffness in patients with nonalcoholic fatty liver disease. *J Hepatol* 2011; 55: 666–72.
- Williams AL, Hoofnagle JH. Ratio of serum aspartate to alanine aminotransferase in chronic hepatitis. Relationship to cirrhosis. *Gastroenterology* 1988; 95: 734–9.
- Wai CT, Greenson JK, Fontana RJ *et al.* A simple noninvasive index can predict both significant fibrosis and cirrhosis in patients with chronic hepatitis C. *Hepatology* 2003; 38: 518–26.
- Lin ZH, Xin YN, Dong QJ *et al.* Performance of the aspartate aminotransferase-to-platelet ratio index for the staging of hepatitis C-related fibrosis: an updated meta-analysis. *Hepatology* 2011; 53: 726–36.
- Sterling RK, Lissen E, Clumeck N *et al.* Development of a simple noninvasive index to predict significant fibrosis in patients with HIV/HCV coinfection. *Hepatology* 2006; 43: 1317–25.
- Vallet-Pichard A, Mallet V, Nalpas B *et al.* FIB-4: an inexpensive and accurate marker of fibrosis in HCV infection. comparison with liver biopsy and fibrotest. *Hepatology* 2007; 46: 32–6.
- Tamaki N, Kurosaki M, Tanaka K *et al.* Noninvasive estimation of fibrosis progression overtime using the FIB-4 index in chronic hepatitis C. *J Viral Hepat* 2013; 20: 72–6.
- Friedrich-Rust M, Ong MF, Herrmann E *et al.* Real-time elastography for noninvasive assessment of liver fibrosis in chronic viral hepatitis. *AJR Am J Roentgenol* 2007; 188: 758–64.
- Morikawa H, Fukuda K, Kobayashi S *et al.* Real-time tissue elastography as a tool for the noninvasive assessment of liver stiffness in patients with chronic hepatitis C. *J Gastroenterol* 2011; 46: 350–8.
- Koizumi Y, Hirooka M, Kisaka Y *et al.* Liver fibrosis in patients with chronic hepatitis C: noninvasive diagnosis by means of real-time tissue elastography – establishment of the method for measurement. *Radiology* 2011; 258: 610–17.

- 21 Tatsumi C, Kudo M, Ueshima K *et al.* Non-invasive evaluation of hepatic fibrosis for type C chronic hepatitis. *Intervirology* 2010; 53: 76–81.
- 22 Tomeno W, Yoneda M, Imajo K *et al.* Evaluation of the Liver Fibrosis Index calculated by using real-time tissue elastography for the non-invasive assessment of liver fibrosis in chronic liver diseases. *Hepatol Res* 2012; 12: 12023.
- 23 Bedossa P, Poynard T. An algorithm for the grading of activity in chronic hepatitis C. The METAVIR Cooperative Study Group. *Hepatology* 1996; 24: 289–93.
- 24 Castera L, Foucher J, Bernard PH *et al.* Pitfalls of liver stiffness measurement: a 5-year prospective study of 13,369 examinations. *Hepatology* 2010; 51: 828–35.
- 25 Fraquelli M, Rigamonti C, Casazza G *et al.* Reproducibility of transient elastography in the evaluation of liver fibrosis in patients with chronic liver disease. *Gut* 2007; 56: 968–73.
- 26 Arena U, Vizzutti F, Abraldes JG *et al.* Reliability of transient elastography for the diagnosis of advanced fibrosis in chronic hepatitis C. *Gut* 2008; 57: 1288–93.
- 27 Rizzo L, Calvaruso V, Cacopardo B *et al.* Comparison of transient elastography and acoustic radiation force impulse for non-invasive staging of liver fibrosis in patients with chronic hepatitis C. *Am J Gastroenterol* 2011; 106: 2112–20.
- 28 Colombo S, Buonocore M, Del Poggio A *et al.* Head-to-head comparison of transient elastography (TE), real-time tissue elastography (RTE), and acoustic radiation force impulse (ARFI) imaging in the diagnosis of liver fibrosis. *J Gastroenterol* 2012; 47: 461–9.
- 29 Ferraioli G, Tinelli C, Dal Bello B, Zicchetti M, Filice G, Filice C. Accuracy of real-time shear wave elastography for assessing liver fibrosis in chronic hepatitis C: a pilot study. *Hepatology* 2012; 56: 2125–33.

特集II B型肝炎の概念の変遷とその臨床的意義

B型肝炎ウイルスジェノタイプB 高感染地域における感染実態の 変遷と核酸アナログ治療例に おけるジェノタイプの臨床的意義*

渡辺久剛**
佐藤智佳子**
奥本和夫**
西瀬雄子**
斎藤貴史**
河田純男***
上野義之**

Key Words: HBV genotype, HBV carrier, acute hepatitis, nucleotide analogue

はじめに

わが国において、B型肝炎ウイルス(HBV)感染者のHBVジェノタイプは、全体の80%以上を占めるC型がメジャータイプであるが、その分布には地域特性が知られている¹⁾。これまでの後ろ向きコホート研究から、山形県は全国有数のHBVジェノタイプBの高感染地域であることを報告してきた²⁾。

また、HBVジェノタイプA型感染によるB型急性肝炎は都市部においてその広がりが増加している³⁾、地方においても増加傾向にあるものと推測され、今後の感染拡大が予想される。そのような症例では肝炎の遷延化も指摘されており⁴⁾、ユニバーサルワクチン導入の是非を議論する上でも、その感染実態を把握することは重要である。HBVジェノタイプB型高浸淫地域における、最近のB型急性肝炎のジェノタイプによる感染実態は明らかではないことから、過去20年間の当地域のHBVキャリアおよび急性肝炎例のHBVジェノタイプ別感染の変遷を検討した。

一方、B型慢性肝疾患に対する抗ウイルス治

療は、現在、核酸アナログ製剤(NA)が主流であるが、ペグインターフェロンの保険適用に伴い、今後NA治療患者からの切り替え例が増えてくるものと予想される。しかし、NA中止に伴う肝炎再燃のリスクもあり、どのような症例でNAを中止できるか議論のあるところである。最近の報告では、NA中止の指標にHBs抗原(HBsAg)とHBコア関連抗原(HBcrAg)量の測定の有用性が示されており⁵⁾、NA治療効果とウイルス抗原量スコア化に基づいたNA中止可能例について、HBVジェノタイプの観点から検討した。

HBVキャリアの

HBVジェノタイプ別感染実態の変遷

1990年から2009年まで、急性肝炎患例を除き、経過追跡可能かつジェノタイプが測定可能であったHBs抗原陽性のHBVキャリア359例を対象とした。NA製剤が保険適用となった2000年を境に、1990年から1999年(237例)、2000年から2009年(122例)の2群に分けて、キャリアにおける各HBVジェノタイプ別の感染頻度の変遷を検討した。

その結果、キャリア全体のジェノタイプの感染頻度は、A型11例(3.1%)、B型194例(54.0%)、C型150例(41.8%)、D型4例(1.1%)であった。前後10年でその頻度を比較すると(図1)、1999

* Hepatitis B virus genotypes in a hyperendemic area for genotype B infection and clinical significance of genotypes in patients with nucleotide analogue treatment.

** Hisayoshi WATANABE, M.D., Chikako SATO, M.D., Kazuo OKUMOTO, M.D., Yuko NISHISE, M.D., Takafumi SAYTO, M.D. & Yoshiyuki UENO, M.D.: 山形大学医学部消化器内科(〒990-9585 山形県山形市飯田西2-2-2); Department of Gastroenterology, Yamagata University School of Medicine, Yamagata 990-9585, JAPAN

*** Sumio KAWATA, M.D.: 兵庫県立西宮病院

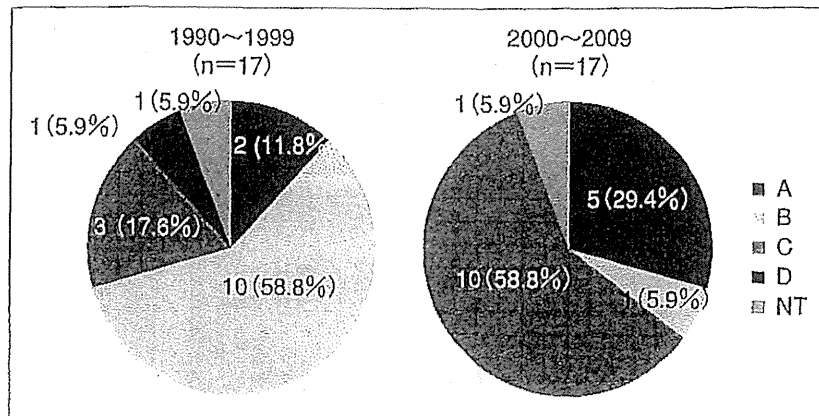


図4 B型急性肝炎におけるジェノタイプの推移(文献⁹より引用)

表2 ジェノタイプA感染による急性肝炎例

Case No.	Age (Years)	Sex	ALT* (IU)	IgM anti-HBc (S/CO)	HIV Ab	HBsAg clearance (months)	Outcome	Treatment	Route of Infection	Genotype
1	45	M	185	10.2	(-)	Persistently positive	chronicity	LAM	heterosexual	Ae
2	22	M	1,282	41.3	(-)	4	resolved	ETV	heterosexual	Ae
3	26	M	2,008	26.3	(-)	9	resolved	ETV	heterosexual	Ae
4	49	F	557	22.6	(-)	5	resolved	-	heterosexual	Ae
5	26	M	3,650	29.9	(-)	3	resolved	-	heterosexual	Ae
6	56	M	2,876	8.3	(-)	3	resolved	-	heterosexual	Ae
7	55	F	1,414	7.2	(-)	5	resolved	-	heterosexual	Ae

LAM : Lamivudine, ETV : Entecavir. * 初診時

(文献⁹より引用)

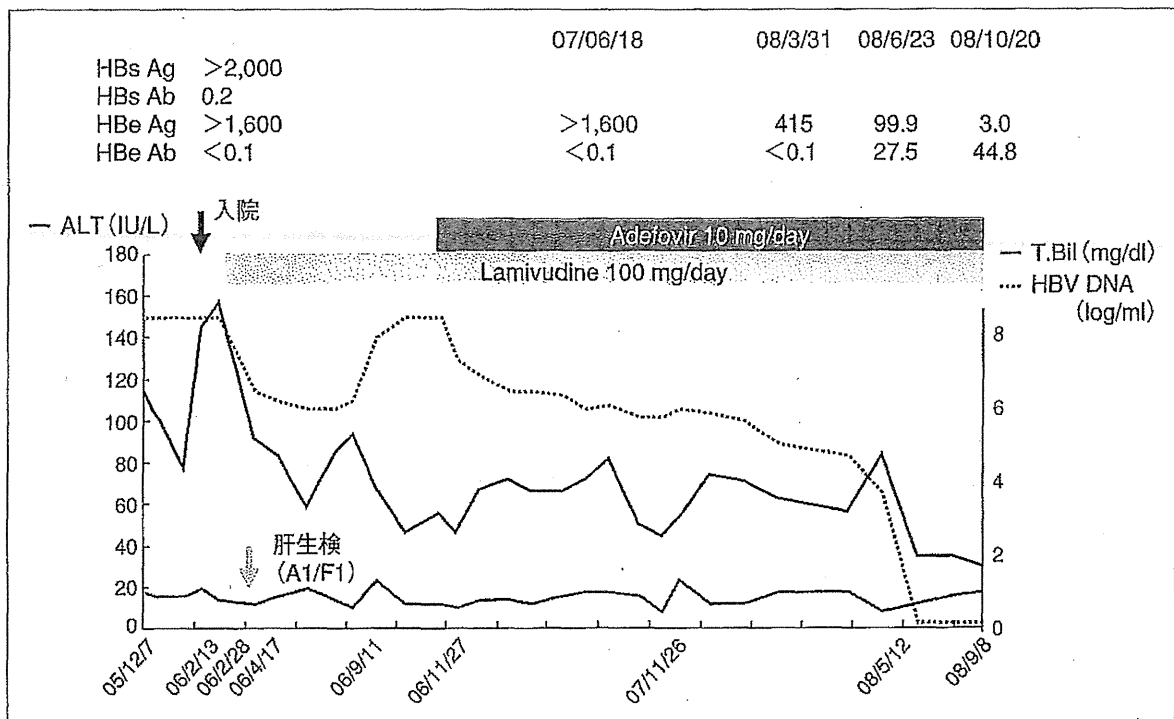


図5 慢性化したB型急性肝炎の1例(Case No.1)

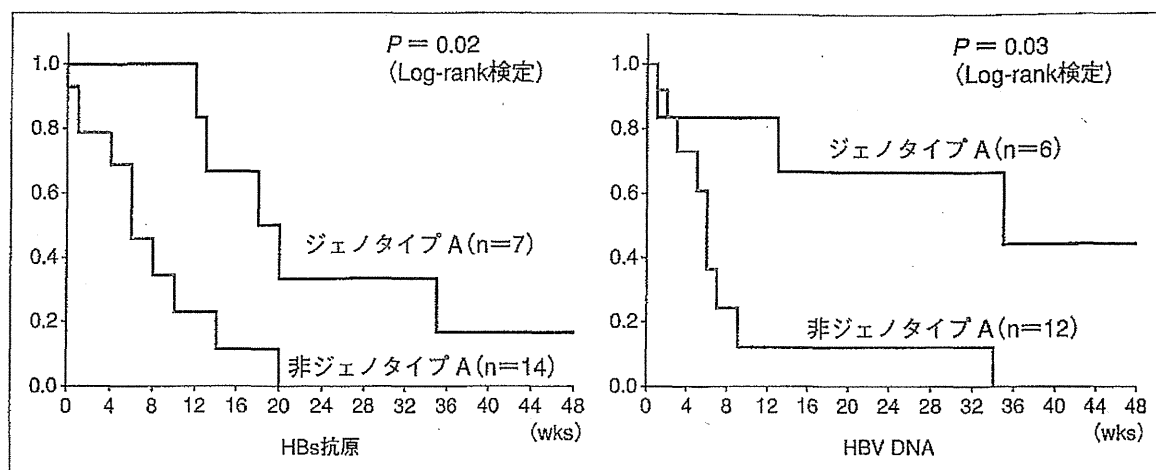


図6 ジェノタイプA, 非A型感染におけるHBs抗原, HBV DNA陰性化時期
HBs抗原陰性化はジェノタイプA型感染例では有意に遅く(49週 vs. 8週; $P < 0.05$), HBV DNA陰性化時期も非A型感染例に比べ有意に遅かった(45週 vs. 4.9週; $P < 0.05$).

場検診ではじめてALT値の上昇とHBs抗原陽性を指摘され, 血清学的にB型急性肝炎と診断された。ラミブジンが投与されたが改善せず, その後ラミブジン耐性ウイルスが出現し, アデフォビルの投与によりALT値とウイルス量の低下を見た。肝機能異常を検診ではじめて指摘されてから約3か月後のラミブジン投与前の肝生検では, すでに慢性肝炎(A1/F1)の組織像を呈していた。他の6例は, 来院時にいずれも急性肝炎に特徴的な症状とALT値の高値を伴い, その後HBs抗原の陰性化を確認している⁷⁾。

HBs抗原陰性化時期を比較すると, ジェノタイプA型感染例では有意に遅く, HBV DNA陰性化時期も非A型感染例に比べ有意に遅かった(図6)。一方, HBe抗原陰性化時期, HBe抗体出現時期, IgM-HBc抗体陰性化時期やALT値正常化時期は差がなかった。

本地域で経験したB型急性肝炎例の検討からは, 1999年以前には半数を占めていたジェノタイプB型感染者が, 最近10年間ではほとんどみられなくなっていることが明らかとなった。従来HBVジェノタイプB型感染者が圧倒的に多い本地域において, ジェノタイプB型感染のB型急性肝炎例に占める割合が2000年以降に急激に低下していることは興味深い。一方, 急性肝炎に占めるジェノタイプC型感染の割合はこの10年間で増加していたが, その理由として, ジェノタイプA型感染の増加と相まって, 本州にお

ける主なジェノタイプであるC型感染も地方へ広がってきているためと推測する。

本検討から, 少なくとも過去にジェノタイプB型感染の頻度が高かった地域においてはジェノタイプB型感染が減少し, ジェノタイプA型感染が確実に増加してきていることが明らかとなった。特に急性期に自覚症状を欠き検診などで偶然に見つかる例にも遭遇することから, 地方におけるジェノタイプA型感染の拡大にも, 今後は十分に留意する必要があるものと思われた。

NA投与例における治療効果およびウイルス抗原量の推移とジェノタイプの関連

NAを2年以上長期投与したB型慢性肝炎患者例について, 開始時および開始2年後のALT値, HBV DNA量, HBsAg量, HBcrAg量を測定し, ジェノタイプによるNA長期内服の治療効果とウイルス抗原量スコア(表3)の推移について検討した。

NAを長期投与したジェノタイプB 28例, ジェノタイプC 31例では, HBV DNA 7 log以上, HBcrAg量 4 log U以上の例がジェノタイプCに有意に多く, NA平均投与期間はジェノタイプCで有意に長かった(53か月 vs. 74か月, $P < 0.01$)。投与2年時のALT正常化率, HBV DNA陰性化率は差がなかったが, HBcrAg陰性化率(< 3.0 log U)は, ジェノタイプB 5/10(50%), ジェノタイプ

表3 HBsAg量とHBcrAg量をもとにしたNA中止による肝炎再燃リスクの予測

HBsAg levels (IU/ml)	Scores	HBcrAg levels (log U/ml)	Scores
<80	0	<3.0	0
80~800	1	3.0~4.0	1
800≤	2	4.0≤	2

↓

Risk of hepatic flare	Total scores	% of prediction success
Low-risk group	0	80~90%
Medium-risk group	1~2	~50%
High-risk group	3~4	10~20%

(文献⁵⁾より引用改変)

C 3/14 (21%)とジェノタイプB例で高かった ($P < 0.05$).

NA開始後2年のウイルス抗原量スコア化による低~中再燃リスク(スコア0~2)を満たす例はジェノタイプBで62%, ジェノタイプCで29% ($P < 0.05$)であった(図7). ウイルス抗原量スコア0~2到達に寄与する因子として, 単変量解析ではNA開始時年齢(HR 1.01, $P = 0.02$)とジェノタイプ(HR 3.11, $P = 0.01$)が関連し, 多変量解析でもNA開始時年齢(HR 1.04, $P = 0.04$)とジェノタイプ(HR 2.96, $P = 0.03$)がそれぞれ独立して寄与する因子であった.

以上よりNA治療反応性はジェノタイプBで良好であり, その結果, ウイルス抗原量スコアリングに基づく再燃リスクが低い例が多かったことから, NA中止あるいはHBsAg消失を目指したpegインターフェロン治療への切り替えにあた

り, ジェノタイプは有用なマーカーの一つであると思われた.

おわりに

ジェノタイプB型高浸淫地域における検討では, HBVキャリア全体のジェノタイプの感染割合は過去と現在で大きな変化はみられなかったが, B型急性肝炎例では地方においてもジェノタイプA型感染が増加していた. ジェノタイプは肝病態の進展と関連しており, 抗ウイルス治療の際のウイルス抗原量の推移にも影響する因子であったことから, B型肝炎の病態・治療においてその臨床的意義は大きいと思われた.

文 献

- 1) Orito E, Ichida T, Sakugawa H, et al. Geographic distribution of hepatitis B virus (HBV) genotype in patients with chronic HBV infection in Japan. *Hepatology* 2001; 34: 590.
- 2) 渡辺久剛, 斎藤貴史, 河田純男. HBV genotype B ハイブリッド遺伝子型(Bj, Ba)の臨床的差異. *肝臓* 2003; 44: A378.
- 3) 山田典栄, 四柳 宏, 小坂橋優, ほか. 首都圏におけるB型急性肝炎の実態と変遷—Genotype Aに焦点をあてて—. *肝臓* 2008; 49: 553.
- 4) Suzuki Y, Kobayashi M, Ikeda K, et al. Persistence of acute infection with hepatitis B virus genotype A and treatment in Japan. *J Med Virol* 2005; 76: 33.
- 5) Tanaka E, Matsumoto A. Guidelines for avoiding risks resulting from discontinuation of nucleoside/

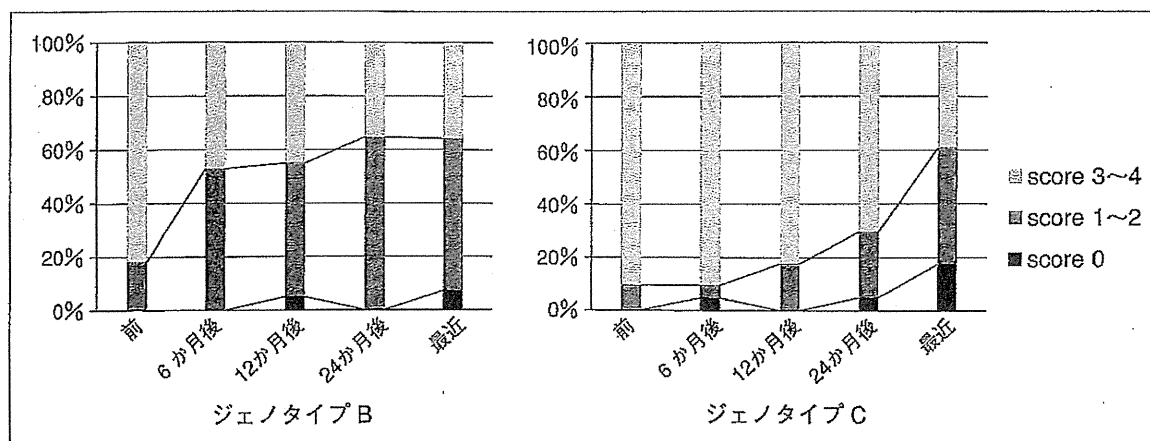


図7 ジェノタイプによるウイルス抗原量総スコアの推移

nucleotide analogs in patients with chronic hepatitis B. *Hepatol Res* 2014 ; 44 : 1.

- 6) 渡辺久剛, 斎藤貴史, 富田恭子, ほか. B型肝炎ウイルスジェノタイプB型感染高浸淫地区における感染実態の変遷. *肝臓* 2011 ; 52 : 753.

- 7) 斎藤貴史. 山形県におけるHBVジェノタイプの分布. 厚生労働省肝炎等克服緊急対策研究事業, 平成21-23年度総合研究報告書. 「B型肝炎ジェノタイプA型感染の慢性化など本邦における実態とその予防に関する研究」. 2012. pp. 319-27.

* * *

Review Article

Application of deep sequence technology in hepatology

Masashi Ninomiya,¹ Yoshiyuki Ueno^{2,3} and Tooru Shimosegawa¹¹Division of Gastroenterology, Tohoku University Graduate School of Medicine, Sendai, ²Department of Gastroenterology, and ³CREST, Yamagata University Faculty of Medicine, Yamagata, Japan

Deep sequencing technologies are currently cutting edge, and are opening fascinating opportunities in biomedicine, producing over 100-times more data compared to the conventional capillary sequencers based on the Sanger method. Next-generation sequencing (NGS) is now generally defined as the sequencing technology that, by employing parallel sequencing processes, producing thousands or millions of sequence reads simultaneously. Since the GS20 was released as the first NGS sequencer on the market by 454 Life Sciences,

the competition in the development of the new sequencers has become intense. In this review, we describe the current deep sequencing systems and discuss the application of advanced technologies in the field of hepatology.

Key words: deep sequencing technology, next-generation sequencing, pyrosequencing, sequencing-by-synthesis

INTRODUCTION

DEEP SEQUENCING TECHNOLOGIES are currently hot topics and are opening fascinating opportunities in the study of biomedicine. They can produce over 100-times more data compared to the traditional capillary sequencers based on the standard Sanger method. This technology was introduced in *Nature Methods* as the method of the year in 2007.¹

In 1975, Sanger first reported the sequencing method by primed synthesis with DNA polymerase.² In 1977, epoch-making articles were published in succession. DNA sequencing for the genome of a bacteriophage was conducted with the Sanger enzymatic dideoxy technique based on chain-terminating dideoxynucleotide analogs.^{3,4} A method of DNA sequencing reported in the same year by Maxam and Gilbert and known as Maxam–Gilbert sequencing involves chemical cleavage at specific bases of terminally labeled DNA fragments and separation by gel electrophoresis.⁵ The automation of DNA sequence analysis was developed by Caltech (California Institute of Technology, Pasadena, CA, USA) and commercialized by Applied Biosystems (ABI,

Applied Biosystems, Foster City, CA, USA), Wilhelm Ansoerge at the European Molecular Biology Laboratory and Pharmacia-Amersham, later General Electric Healthcare (GE Healthcare, Little Chalfont, Buckinghamshire, UK).^{6–8}

The Sanger method was used in the first automated fluorescent DNA sequencing, in which a complete sequence of 57 kb of the human hypoxanthine-guanine phosphoribosyltransferase (*HGPRT*) gene was determined.⁹ ABI introduced the ABI Prism 310 automated DNA sequencer in 1996 and the automated capillary sequencer ABI Prism 3700 in 1998. Together with advances in automation and development of new biochemicals, the Sanger method has made possible the determination of various sequences in many research projects. An initial rough draft of the human genome was finished and announced jointly by US President Bill Clinton and British Prime Minister Tony Blair in 2000, and another study reported the sequencing of the human genome of up to 3 billion bases.^{10,11} The first human genome sequence of the Human Genome Project (HGP) was completed in 2003. The HGP has taken 13 years and cost \$US 2.7 billion. Using the basic dideoxy method of Sanger sequencing enabled a great achievement.

Before the human genome sequence was completed, Venter proposed a project entitled "The Future of Sequencing: Advancing Towards the \$1000 Genome" at the opening session of The Genome Sequencing and

Correspondence: Dr Yoshiyuki Ueno, Department of Gastroenterology, Yamagata University Faculty of Medicine, 2-2-2 Iidanishi Yamagata-shi, Yamagata 990-9585, Japan. Email: y-ueno@med.id.yamagata-u.ac.jp

Received 2 July 2013; revision 2 July 2013; accepted 25 July 2013.

Analysis Conference in 2002 and announced that his foundation would earmark a prize for a breakthrough leading to the goal. Formally, the National Institutes of Health convened the National Human Genome Research Institute and introduced the first in a series of \$1000 Genome grants designed to advance the development of breakthrough technologies in 2004. The reaction at the completion of the human genome sequence was different between Japanese and US scientists. While Japanese was considered to have “finished” sequence technology, the USA was thought to have begun. Therefore, some venture companies competed to develop new sequence technology. In 2000, Rothberg established 454 Life Sciences (Branford, CT, USA) and developed the first next-generation sequencing (NGS) system, the GS instrument, in 2005.^{12,13} In this review, we describe NGS systems and discuss the application of these advanced technologies in hepatology.

FIRST NGS SYSTEMS: 454 GS SERIES

THE NGS IS now generally defined as the sequencing technology that employs parallel sequencing processes producing thousands or millions of sequence reads simultaneously. Rothberg and colleagues first succeeded in sequencing the *Mycoplasma genitalium* genome with 96% coverage and 99.96% accuracy in a single GS20 run.¹³ The GS20 was the first NGS sequencer put on the market by 454 Life Sciences. In the following years, Roche (Basel, Switzerland) absorbed 454 Life Sciences and extended GS20 to a new version of the GS FLX titanium series. The GS FLX titanium series used a parallel pyrosequencing system capable of data output from 100 Mb to 500 Mb per run with a 400–500 bp read length. The pyrosequencing of this sequencer is based on measuring the pyrophosphate generated by the DNA polymerization reaction.^{14,15} DNA is fractionated into the fragments of 300–800 bp and these DNA fragments are ligated with short adapters that contain the binding of one fragment to a streptavidin-coated bead. Emulsion polymerase chain reaction (PCR) is carried out for fragment amplification, with water droplets containing one bead and PCR reagents immersed in oil. When the PCR amplification cycles are completed, denaturation beads carrying single-stranded DNA clones are placed into the wells of a fiber-optic slide. On the slide, amplified DNA bound to each of the beads containing sulfurylase and luciferase are sequenced. When one nucleotide is added to the complementary template by the polymerase reaction, a charge-coupled device (CCD) sensor can record the light signal from luciferin. Of note, the signal

strength is proportional to the number of nucleotides.¹³ This technology is defined as “sequencing-by-synthesis” and is called pyrosequencing in this system.

SECOND-GENERATION NGS SYSTEM: THE ILLUMINA GENOME SEQUENCER

GENERALLY, THE ROCHE/GS FLX titanium series, the Solexa Genome Analyzer (Illumina, San Diego, CA, USA) and the ABI SOLiD system are now classified as second-generation NGS systems. However, the GS FLX series could obtain smaller amounts of data per run than the Illumina or SOLiD systems. Therefore, some technologists believe that Illumina and SOLiD sequencers are second-generation NGS systems.

The Solexa sequencing system, acquired by Illumina, was commercialized in early 2007. The Illumina Genome Analyzer is also based on the “sequencing-by-synthesis” to produce short sequence reads of millions of surface amplified DNA fragments simultaneously. Starting with fragmentation of the genome DNA, adaptor-ligated DNA fragments are attached to the surface of a glass flow cell. The flow cell is separated into eight channels and the surfaces of the channels have covalently attached oligos complementary to the adaptors and ligated to the library DNA fragments. Then, on the flow cell, adaptor-ligated DNA fragments are amplified by polymerase reaction for bridge amplification and form the cluster fragments. The cluster fragments are denatured; annealed with a sequencing primer and subjected to DNA synthesis with four differentially reversible labeled fluorescent nucleotides that have their 3'-end chemical termination to ensure that only a single base is extended. After a single base is incorporated into the DNA strand, the terminator nucleotide is detected via its labeled fluorescent dye by the CCD camera. Then, the labeled fluorescent dye and 3'-end chemical terminations are removed and the next DNA synthesis cycle is repeated.

The Genome Analyzer IIx can obtain 30–100 nucleotide read lengths and data output per paired-end run from 1–3 Gb.^{16–18} Moreover, Illumina released a HiSeq sequencer series which enabled higher throughput and a desktop MiSeq sequencer type which could sequence more rapidly in 2013.

SECOND-GENERATION NGS SYSTEM: THE ABI SOLID SEQUENCER

THE ABI SOLiD sequencer was introduced in October 2007. SOLiD is an abbreviation for “sequencing